Behavior of SNAP-10A during Orbital Re-Entry

DONN K. NELSON*
North American Aviation, Inc., Canoga Park, Calif.

The system for nuclear auxiliary power (SNAP 10A) is a power system that uses thermoelectric elements to convert the heat developed by a compact nuclear reactor into electrical energy. The present analysis begins at an altitude in the process of satellite orbit decay where the satellite will not make another complete circuit of the oblate, rotating earth. Results show that the SNAP 10A vehicle has aerodynamic stability with the reactor pointed forward into the airstream and oscillates about the flight path during re-entry. The amplitude and frequency of these oscillations are analyzed with respect to time and altitude for a system with two degrees of freedom. The transient heating of the reactor system results in ablation of the forward section of the reactor and adjacent lightweight components at altitudes near 300,000 ft. The heavier components with greater heat capacity and some parts previously shielded rise in temperature until the reactor separates from the SNAP 10A system. This event is followed by individual fuel element release at about 240,000 ft.

Nomenclature

A = reference area, ft²
a = thermal accommodation coefficient
C_A = axial force coefficient, $C_A = F_A/qA$
CAP = thermal capacity of a specified node, Btu/°F
C_D = drag coefficient, $C_D = F_D/qA$
c.g. = center of gravity
C_K = mass fraction of component K
C_m = pitching moment coefficient, $C_m = M_y/qAL$
C_N = normal force coefficient, $C_N = F_N/qA$
C_{rad} = radiation heat-transfer coefficient [Eq. (5)], Btu/sec-°F
C_{cond} = conduction heat-transfer coefficient [Eq. (5)], Btu/sec-°F
d = diameter, ft
H = enthalpy, Btu/lb
H_{D_e} = energy in dissociation, $H_{D_e} = \sum_k [C_k i_k^\circ]_e$, Btu/lb
i_k° = heat evolved in the formation of component k at 0°F per unit mass
I_{yy} = pitch moment of inertia, slug-ft²
J = mechanical equivalent of heat, 778 ft-lb/Btu
K_n = Knudsen number
L = body length, ft
M_y = pitching moment, ft-lb
Pr = Prandtl number
Q = aerodynamic heating rate to a particular node, Btu/sec
q = dynamic pressure, psf
q = heating rate, Btu/ft²-sec
Re = Reynolds number, $Re = \rho_e V_e x/\mu_e$
Rn = spherical nose radius, ft
T = temperature
V = velocity, fps
W = weight, lb
x = distance measured from leading edge, ft
α = vehicle angle of attack, deg
γ = flight angle, deg
θ = angle between any radius vector and the radius vector parallel to freestream flow, deg
μ = viscosity, lb-sec/ft²
ρ = atmospheric density, slugs/ft³
τ = time, sec
φ = latitude, deg

Subscripts

c = circular satellite condition
e = conditions at the edge of boundary layer
FM = free molecular heat-transfer conditions
node = particular element of material
SL = sea level conditions
STAG = stagnation-point conditions
w = conditions at the wall
∞ = freestream conditions
540 = enthalpy level at 540°R

Introduction

BEFORE orbital testing and subsequent use of SNAP 10A (Fig. 1), any potential radiological problems affecting public health and safety must be evaluated. Only those problems associated with re-entry of the SNAP 10 A system are discussed herein. The reactor will be subcritical at launch. Criticality can be achieved only by activating the beryllium control drums or immersion of the reactor assembly in a moderating material such as water. Reactor start-up will be initiated only after the system has been placed in the proper orbit. Therefore, the behavior of the SNAP 10A-Agena vehicle (an Atlas-Agena launch vehicle is proposed) during re-entry becomes a prime consideration.

Electrical power is generated by SNAP 10A as a result of heat flow through thermoelectric elements with rejection to the space environment.[1] Circulating liquid metal (a sodium-potassium alloy, NaK-78) in the system transfers the heat generated by the reactor to the thermoelectric elements. The reactor subsystem (Fig. 2) includes the beryllium reflector structure, reactor support legs, thermoelectric pump, and radiation shield. Active reactor control is effected by four mov-

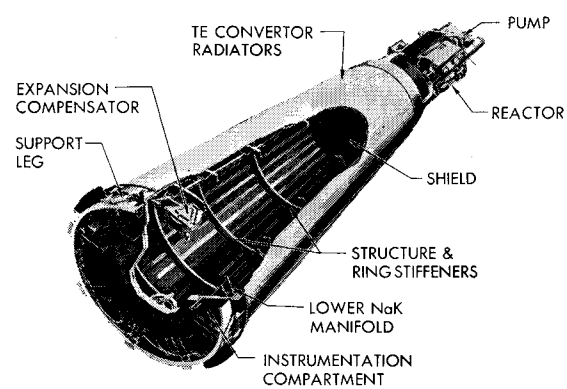

Fig. 1 SNAP 10A system.

Presented as Preprint 64 473 at the 1st AIAA Annual Meeting, Washington, D. C., June 29–July 2, 1964; revision received March 15, 1965. Work described in this paper was performed under Atomic Energy Commission Contract No. AT(11-1)-GEN-8. The author wishes to thank Paul D. Arthur, Consultant and Adjunct Professor of Aerospace Engineering, University of Southern California, for his recommendations in the analysis.

* Senior Engineer, Research, SNAP 10A/2 Reactor Engineering Group, Atomics International Division. Member AIAA.

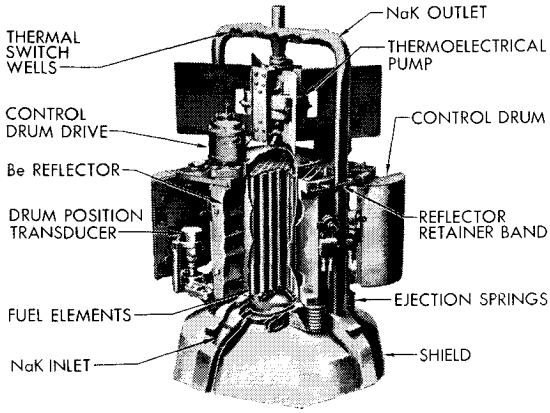

Fig. 2 SNAP 10A reactor.

able drums in the reflector assembly. These drums are used only during reactor start-up, steady-state control being passive; that is, control is based on reactor temperature coefficient. A radiation shield is located directly below the reactor to protect electronic hardware in the instrumentation compartment. The reactor core comprises a hexagonal array of 37 fuel elements surrounded by beryllium reflectors within a cylindrical vessel. The fuel material is a hydrided zirconium uranium alloy.

The SNAP 10A-Agena vehicle is expected to be launched into polar orbit from the Pacific Missile Range. The proposed 700-naut-mile circular orbit (Fig. 3) is accomplished by transfer at the apogee of the elliptical orbit. Because of the significant weight and configuration changes, the following items are important in the re-entry analysis: release of the reflector assembly, reactor separation caused by aerodynamic heating and burn through of the liquid metal (NaK) piping and reactor support legs, and SNAP 10A separation from the Agena vehicle.

Flight Mechanics

The SNAP 10A-Agena vehicle has an orbital lifetime of approximately 3500 years, during which natural orbit decay occurs.[2] When the sensible atmosphere is reached at about 400,000 ft, the satellite will not make another complete circuit of the earth because of the energy dissipated in aerodynamic drag. Since the maximum vehicle orbital altitude occurs at the poles, the initial conditions for this evaluation are defined

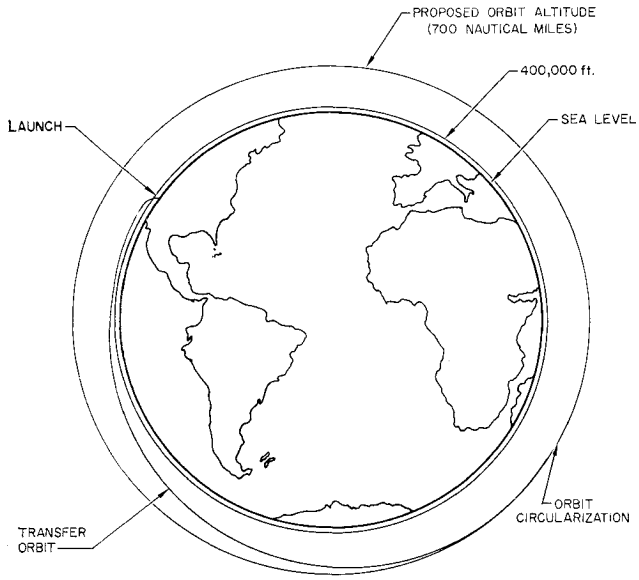

Fig. 3 Typical polar orbit-SNAP 10A.

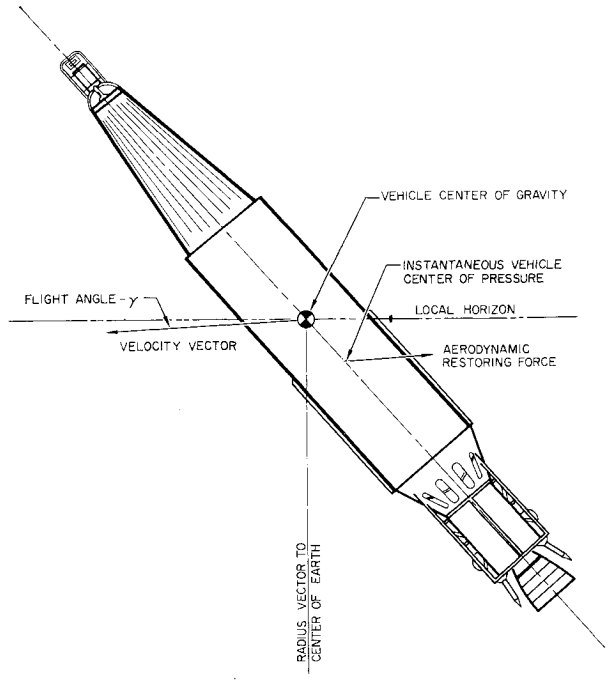

Fig. 4 SNAP 10A-Agena configuration during re-entry.

at an altitude of 400,000 ft over the North Pole. During re-entry (Fig. 4), the resultant of aerodynamic forces imposes a moment that tends to force the vehicle toward zero angle of attack. Therefore, the vehicle oscillates about the center of gravity with the reactor forward in the airstream.

Re-entry trajectory calculations were performed on an electronic digital computer (IBM 7094) using the computer code "RESTORE" developed by Sanders of Atomics International. The equations of motion written in the RESTORE computer code are integrated over an oblate rotating earth. Atmospheric densities used in the calculations are based on the 1962 U. S. Standard Atmosphere.[3]

A representative re-entry trajectory is shown in Fig. 5, together with a reference orbit describing altitude variation caused by earth oblateness in the absence of drag forces. The significant events that occur during re-entry are 1) transition to continuum flow, 2) reactor separates from SNAP system, and 3) SNAP 10A separates from Agena vehicle.

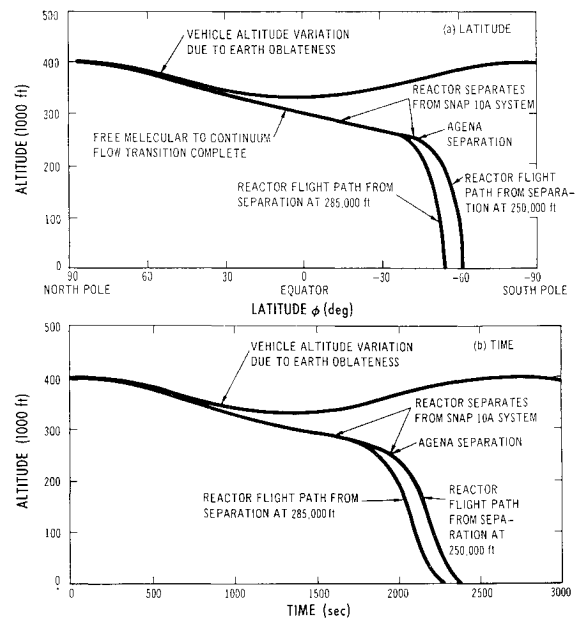

Fig. 5 SNAP 10A re-entry from 400,000 ft over north pole.

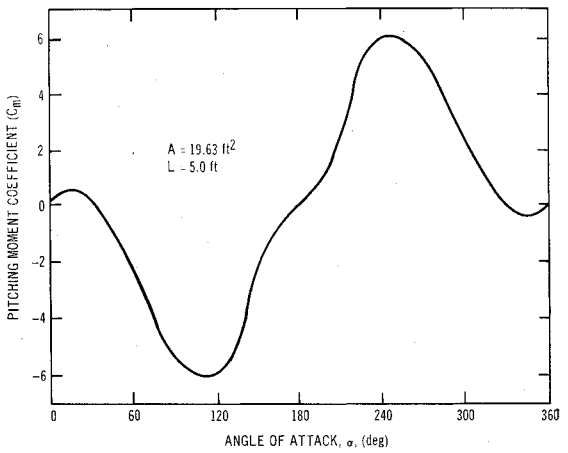

Fig. 6 SNAP 10A-Agena pitching moment coefficient.

These events are presented with respect to altitude and time in Figs. 5a and 5b, respectively. The vehicle enters the atmosphere with an angular rate and arbitrary angle of attack as a result of attitude control. Antenna orientation during system operation requires that the SNAP 10A-Agena make one revolution per orbit, resulting in the reactor always facing outward from the earth.

Aerodynamic forces are exerted on the vehicle depending upon the nature of the flow regime and vehicle angle of attack. The dividing line between slip and continuum flows was taken at a Knudsen number of 0.01. Therefore, the initial portion of re-entry is in free molecular flow, whereas continuum flow pertains below 300,000 ft.

The oscillations of the re-entry vehicle with respect to time (also altitude) along the re-entry trajectory were calculated based on a body having two degrees of freedom. The derivative of vehicle angular rate can be related to the aerodynamic moment and vehicle moment of inertia for this case by the equation

$$(d/d\tau)(d\alpha/d\tau) = M_y/I_{yy} \tag{1}$$

The aerodynamic moment M_y is expressed as

$$M_y = C_m ALq \tag{2}$$

The pitching moment cofficient C_m (Fig. 6) was evaluated with respect to vehicle angle of attack by use of Newtonian theory, as appropriate for the continuum flow regime. In order to compute the aerodynamic coefficients of the re-entering vehicle, the vehicle was broken into separate components where expressions developed by Grimminger, Williams, and Young[4] and Wells and Armstrong[5] were applied. The derived coefficients subsequently have been verified by wind-tunnel testing at Ling-Temco-Vought, Inc. where the operating conditions of the hypervelocity wind tunnel was Mach 17 at an altitude simulation of 250,000 ft. The normal-force coefficient is shown in Fig. 7 where good agreement of experimental results[6] and Newtonian theory is seen for this vehicle configuration.

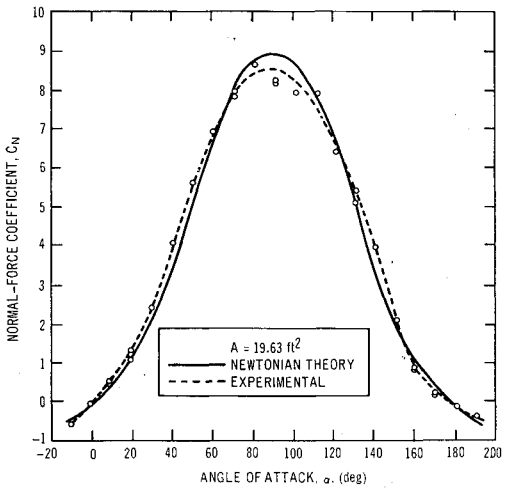

Fig. 7 SNAP 10A-Agena normal-force coefficient.

The aerodynamic moment tends to restore the SNAP 10A-Agena vehicle to a position with the reactor aligned forward along the flight path for angles of attack greater than 30°. The SNAP 10A-Agena vehicle oscillation envelope, cycle frequency, and dynamic pressure for this re-entry case are shown in Fig. 8 for the case where initial vehicle angle of attack is 90°. The reduction in oscillation amplitude and increase in frequency is a pseudodamping provided by the increase in dynamic pressure throughout the orbital decay period to an altitude below significant aerodynamic heating. The increase in dynamic pressure is the result of atmospheric density, which increases monotonically during re-entry.

The ballistic parameter (W/C_DA) of the SNAP 10A-Agena vehicle varies with angle of attack, and consequently with time, during re-entry. The variation is from 1270 to 28 psf at 0° and 90° angle of attack, respectively. The calculation of the re-entry trajectories in Fig. 5 reflects the change in ballistic parameter caused by the damping of vehicle oscillations and component separation.

Re-Entry Heating

The re-entry trajectories and oscillation calculations shown in Figs. 5 and 8, respectively, provided the freestream flight conditions and spatial orientation of the vehicle with respect to time, or altitude, for correlation of aerodynamic heating on vehicle components. During the early re-entry period, the dimensions of some forward reactor components are such that free molecular heating regime persists, so that

$$\dot{q}_{FM} = a\rho V^3/2J \tag{3}$$

The reference heating rate in the continuum regime was defined by the laminar spherical stagnation-point heating rate for a 1-ft-radius sphere. The semi-empirical equation used to

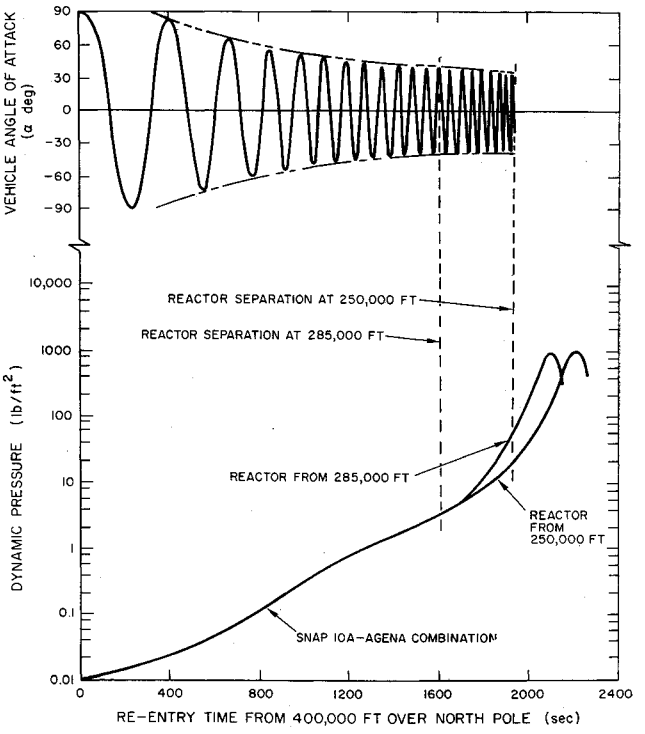

Fig. 8 SNAP 10A-Agena oscillation envelope and dynamic pressure during re-entry.

calculate the heating rate is

$$\dot{q}_{stag} = \frac{17{,}015}{(Rn^{0.5})}\left(\frac{\rho}{\rho_{SL}}\right)^{0.5}\left(\frac{V}{V_c}\right)^{3.0}\left(\frac{H_\infty - H_W}{H_\infty - H_{540}}\right) \quad (4)$$

This equation is the result of modifying the equation derived by Detra and Hidalgo[7] from Fay and Riddell[8] to give vehicle velocity as a fraction of circular satellite velocity. The spherical stagnation-point heating rate for a cold wall (540°R) and vehicle velocity relative to the atmosphere are presented in Fig. 9 for reference.

The liquid metal (NaK) will be contained within the system until meteoroid penetration of the piping or some other form of system rupture occurs. Therefore, for a long orbit lifetime (approximately 3500 yr) it is very likely that the system will re-enter devoid of NaK. The re-entry events for both a system devoid of NaK and a NaK-filled system are described in the following paragraphs.

Re-Entry of a System Devoid of NaK

Normally, ejection of the reflector assembly is initiated after one year of operation, which in turn causes reactor shutdown in orbit after useful system life. This event is initiated by an electrical actuator that severs the retaining band that holds the reflector assembly in the normal operating position. In the event that the reflector assembly is attached at the time of re-entry, the retainer band will be aerodynamically heated to a temperature where separation occurs, releasing the reflector assembly. To be conservative, this analysis considers the reactor re-entering with the reflectors in place.

During re-entry, the band temperatures oscillate because of the variable aerodynamic heating rate being applied to a changing projected band surface area and cyclic reactor shadows on the band. The retainer band will have cycled through the melting temperature of stainless steel by an altitude of 290,000 ft. When the band parts, the reflectors fall away from the reactor vessel, being retained only by a cable harness containing electrical connections and reflector instrumentation. Once ejected, the reflectors will pivot until they contact the reactor support legs and the tip of the shield. In

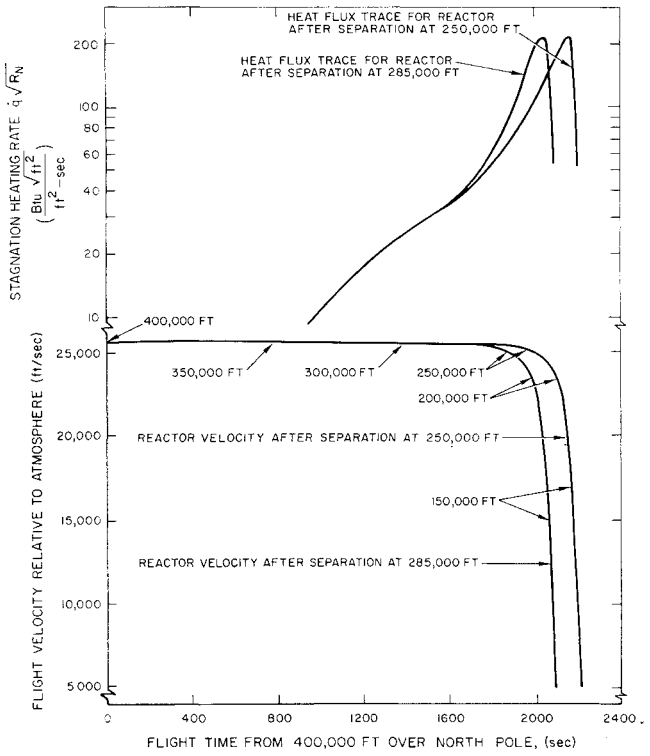

Fig. 9 Continuum regime heating rate and flight velocity profile.

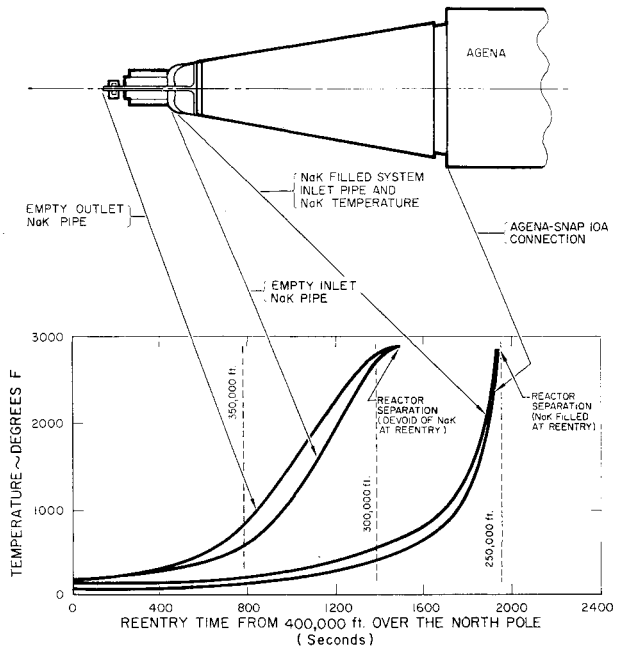

Fig. 10 SNAP 10A temperature profiles during re-entry from orbit.

this position, the cable harness is exposed to aerodynamic heating on the large exposed surfaces of the reflector, with complete release of the reflectors expected to be above 285,000 ft. The equation describing the transient temperature response of an arbitrary node located in the band is

$$T_{node}|_{\tau+\Delta\tau} = T_{node}|_{\tau} + \{C_{rad}T_{space} + C_{rad}T_{reactor} + \Sigma C_{cond}T_{node(adjacent)} + Q - T_{node}(C_{rad,\,space} + C_{rad,\,reactor} + \Sigma C_{cond})\}\Delta\tau/CAP_{node} \quad (5)$$

Separation of the reactor from the SNAP 10A system depends on ablation of the four titanium support legs and the NaK inlet and outlet pipes. The forward portion of the NaK outlet pipe will receive the greatest heating rate of these components during re-entry and will melt through at 290,000 ft. The transient temperature response of the cylindrical section was evaluated by subdivision into nodes similar to the retainer band analysis. The distribution of aerodynamic heating around the body was evaluated by the empirical relation

$$\dot{q} = \dot{q}_{max}\cos^m\theta \quad (6)$$

where the exponent m influences the heating function around the body through the cosine function. Appropriate values of m are between 1.0 and 1.5, depending upon the flow regime.

During melting of the outlet pipes, the reactor remains attached to the converter structure by four titanium support legs that follow the outline of the top of the shield. Shortly after the outlet pipes melt, the 0.032-in.-thick titanium wall melts exposing the portion of the stainless steel NaK inlet lines where the walls are 0.020 in. thick. The effect of the body shapes with differing radii of curvature in perpendicular planes (ellipsoidal, cylindrical) were evaluated by the method described in Ref. 9. Here the stagnation heating rate with respect to body shape in the continuum regime is expressed as

$$\dot{q}_{stag} = \left(\frac{1.00 + 0.38K}{1.38}\right)\dot{q}_{stag,\,3\text{-dimensional}} \quad (7)$$

where K is the ratio of the smaller radius to the larger radius. The maximum transient temperatures of the NaK lines are given in Fig. 10. Ablation of the reactor inlet NaK lines is complete by 285,000 ft. At this point, the reactor will separate from the converter structure and begin to tumble.

The SNAP 10A converter structure-Agena complex remains aerodynamically stable after reactor separation and continues

to re-enter in an oscillating nose forward mode. The aerodynamic heating rate continues to increase after reactor separation, as shown in Fig. 9, burning away the converter structure and severely heating the SNAP 10A-Agena connector ring. The connector will fail by 250,000 ft providing breakup of the vehicle into segments of unknown stability. The heat transfer to the flat thermoelectric converter structure, where transition from laminar to turbulent flow has occurred, was calculated from the correlation given in Ref. 10:

$$\dot{q} = \frac{0.029\ \rho_e V_e (H_e - H_w)[1.00 + 0.04\ (H_{De}/H_e)]}{(Pr)^{0.667}(Re)^{0.2}} \quad (8)$$

The transient temperature response of the SNAP 10A system components during re-entry were evaluated using a thermal analyzer program developed at Atomics International for use on an electronic digital computer.

NaK-Filled System at Re-Entry

The presence of NaK in the SNAP 10A system will retard re-entry ablation by absorbing a portion of the available aerodynamic heat production. A conservative analysis therefore must be based on a configuration with reflectors in place, and a NaK system that has not been penetrated prior to re-entry and which has a flow rate, probably in the reverse direction of operation, as a result of aerodynamic heating of the thermoelectric pump radiator fins.

The NaK system will be simultaneously heated at four principal points: 1) the reactor outlet lines at the forward end of the power unit normal to the flight path, 2) the reactor outlet lines where they penetrate the vessel support legs, 3) the converter tubes, and 4) the upper converter manifold. Heating is greatest where the lines are aligned normal to the air stream; the first penetration will be made at the outlet lines ahead of the reactor. The entire reactor system will heat up as a result of NaK circulation transmitting the heat from local points where aerodynamic heating supplies energy to the system. The average temperature of the system where NaK is flowing is shown in Fig. 10. The NaK in the system has no effect on the reflector retainer band, and reflector ejection again will occur above 285,000 ft.

The event of reactor separating from the remainder of the SNAP 10A system is delayed because of the removal by the flowing NaK of the necessary energy to raise the NaK inlet and outlet pipes to their melting temperatures. The four titanium support legs will melt, exposing the NaK inlet lines to the air stream, thus resulting in NaK line ablation when the NaK system ruptures. Separation of the reactor from the remainder of the system is expected to occur by 250,000 ft as a result of forward NaK pipe burnthrough. Complete ablation of the thermoelectric pump fins and loss of magnetism in the pump by 280,000 ft will result in termination of NaK flow. The temperature of the NaK lines exposed to aerodynamic heating will rise sharply, since heat will no longer be carried away in quantity by the flowing NaK. The most probable point of first penetration will be at the forward NaK lines because of the magnitude of aerodynamic heating at this location. However, system rupture is assured by rupture of an expansion compensator (Fig. 1) placed in the system to allow for NaK volume changes. The expansion compensator will fail at a pressure between 100 to 200 psi (1900° to 2200°F). NaK system rupture, followed by NaK line burnthrough and reactor separation, will occur above 250,000 ft.

Reactor Vessel Ablation

The freely tumbling reactor vessel trajectories begin at 285,000 and 250,000 ft for the respective systems, depending on whether NaK is absent or contained at entry (Fig. 5). The heating of the reactor vessel during the tumbling mode will be greatest at the upper and lower circumferences of the vessel. Since the lip weld on the vessel head has been exposed to aerodynamic heating from the beginning of re-entry, it will be the first part of the vessel to experience complete peripheral melting. The reactor vessel completely ablates by 240,000 ft for both the cases of NaK in the core and core devoid of NaK at the initiation of the re-entry sequence. This is caused by the respective energy (temperature) levels of the reactors at separation. The reactor separated at 285,000 ft has a comparatively cool interior, on the order of 200°F, whereas the reactor separated at 250,000 ft has been heated in excess of 1200°F because of NaK circulation.

The individual fuel elements in the reactor core (Fig. 2) separate and continue on independent trajectories from the point where the vessel is completely melted. The release of fuel elements from this altitude (240,000 ft) in the re-entry trajectory exposes the fuel to a major portion of the available aerodynamic heating. The ballistic parameter (W/C_DA) of an individual fuel element has a value between 20 and 30 for crossflow orientation with oscillations. Therefore, deceleration will take place during a sufficiently long time interval to impart appreciable aerodynamic heating to a fuel element.

Table 1 SNAP 10A-Agena separation summary

Item	System devoid of NaK at re-entry: Time,[a] sec	System devoid of NaK at re-entry: Altitude, ft	System with NaK circulation: Time,[a] sec	System with NaK circulation: Altitude, ft
NaK outlet pipe (front of reactor)	1540	290,000	1950	250,000
Retainer band rupture, reflector ejection[b]	1720	285,000	1720	285,000
Reactor support legs	1720	285,000	1720	285,000
NaK system loop rupture	..	....	1760	275,000
NaK inlet pipe (at support legs) reactor separation from SNAP 10A system	1720	285,000	1950	250,000
Agena separation	1890	245,000	1970	245,000
Reactor vessel ablation (fuel element release)	1900	240,000	1990	240,000
Impact	2260	Sea level	2370	Sea level

[a] Time zero at 400,000 ft over North Pole.
[b] If not previously ejected at the time of reactor shutdown in orbit.

Concluding Remarks

Ablation of the vehicle during re-entry results in component separation and exposure of the nuclear fuel to direct aerodynamic heating. The results of this study indicate that, with release of fuel elements at an altitude of 240,000 ft, a major fraction of the aerodynamic heat pulse remains for fuel burnup during re-entry. The results of this study are at present being correlated to data gathered on the RFD-1 test (reactor flight demonstration—no. 1, conducted jointly by the Sandia Corporation and Atomics International for the Atomic Energy Commission) and fuel ablation experiments conducted under the aerospace safety program at Atomics International. The separation sequences of the SNAP 10A (void or filled NaK systems at re-entry) as described in this paper are listed in Table 1 for reference.

References

[1] Anderson, G. M., "Nuclear reactor systems," Astronaut. Aerospace Eng. 1, 27–36 (May 1963).

[2] Elliott, R. D., "Aerospace safety reentry analytical and experimental program SNAP 2 and 10A," North American Aviation Rept. SR-8303 (September 30, 1963).

[3] Dubin, M., Sissenwine, N., and Wexler, H., *U. S. Standard Atmosphere, 1962* (Government Printing Office, Washington D. C., 1962).

[4] Grimminger, G., Williams, E. P., and Young, G. B. W., "Lift on inclined bodies of revolution in hypersonic flow," J. Aeronaut. Sci. **17**, 675–690 (1950).

[5] Wells, W. R. and Armstrong, W. O., "Tables of aerodynamic coefficients obtained from developed Newtonian expressions for complete and partial conic and spheric bodies at combined angles of attack and sideslip with some comparisons with hypersonic experimental data," NASA TR R-127 (1962).

[6] Lindsey, J. L., "Ling-Temco-Vought hypervelocity wind tunnel force and dynamic stability test for the SNAP 10A-Agena configuration," Hypervelocity Wind Tunnel Test 28 (April 1965).

[7] Detra, R. W. and Hidalgo, H., "Generalized heat transfer formulas and graphs for nose cone reentry into the atmosphere," ARS J. **31**, 318–321 (1961).

[8] Fay, J. A. and Riddell, F. R., "Theory of stagnation point heat transfer in dissociated air," J. Aeronaut. Sci. **25**, 73–85 (1958).

[9] Reshotko, E., "Heat transfer to a general three-dimensional stagnation point," Jet Propulsion **28**, 58–60 (1958).

[10] Rose, P. H., Probstein, R. F., and Adams, Mac C., "Turbulent heat transfer through a highly cooled, partially dissociated boundary layer," J. Aeronaut. Sci. **25**, 751–760 (1958).

SEPT.-OCT. 1965 J. SPACECRAFT VOL. 2, NO. 5

Applications of Snap-50 Class Powerplants to Selected Unmanned Electric Propulsion Missions

W. R. Fimple* and T. N. Edelbaum†
United Aircraft Research Laboratories, East Hartford, Conn.

The mission applications include: solar, Jupiter, and Saturn probes, a Venus satellite, and a continuous lunar logistic supply operation. General results of payload fraction vs mission time for the interplanetary missions are presented in plots containing contours of constant thruster efficiency and specific impulse. These plots may be used with good accuracy to evaluate any thruster with a known variation of efficiency with specific impulse. Performance comparisons are made between electric and solid-core nuclear rocket propulsion for all of the missions. A general conclusion of the study is that a powerplant specific weight of less than 30 lb/kwe must be achieved in order for electric propulsion to compete with nuclear rockets in the 700 to 900 sec range of specific impulse. It is also shown that electric propulsion devices having a specific impulse of less than 3000 sec are not competitive with either nuclear rockets or ion engines even if they can achieve high efficiency. The results for the lunar supply operation show that electric propulsion is superior to nuclear rockets on a performance basis and that the two systems are competitive on a specific cost basis.

Introduction

If a program of unmanned space missions includes missions that differ greatly in degree of difficulty, no one type of propulsion can be expected to be clearly superior for all of them. Since it may be impractical and too expensive to develop specific advanced propulsion vehicles for each mission, the final choice may be a compromise system capable of performing each of the missions well but not necessarily better than other contenders.

Barring any unforeseen breakthroughs in the possible development of gas-core nuclear rockets or nuclear-pulse rockets, the only propulsion systems that could be available in the 1970's for unmanned exploration of the solar system are chemical rockets, solid-core nuclear rockets, and nuclear-electric rockets. For unmanned scientific interplanetary missions, such as probes to the major planets and the sun, chemical rockets are at best only marginally adequate. Another difficult unmanned mission is a lunar logistic supply operation; although the lunar supply operation can be performed with chemically propelled vehicles, it could certainly be done more efficiently and economically using more advanced propulsion.

The aim of this study was to evaluate the potentials of solid-core nuclear rockets and nuclear-electric propulsion as candidates for a compromise propulsion system for five selected unmanned missions that are representative of the range of difficulty of a whole program of unmanned missions. These are a Venus orbiter, Jupiter, Saturn, and solar probes, and a lunar logistic supply operation.

Some of the more significant previous mission studies of electric propulsion are listed as Refs. 1–12. It is believed that the present paper represents a significant contribution to this class of studies for the following reasons: 1) it presents a complete comparison of the respective payload capabilities of solid-core nuclear rockets and nuclear-electric propulsion for the representative missions covering a range of specific impulse and powerplant specific weights, 2) the electric-propulsion performance results for the interplanetary missions can be applied within limits to any launcher and thruster, and 3) the comparative economic results for the lunar logistic supply operation have not been presented before.

Definitions and Ground Rules

Space Vehicles

Electrically propelled vehicles

The initial gross weight of an electrically propelled vehicle is considered to be composed of the following: powerplant (including power conditioning equipment and shielding), thruster, propellant tanks, propellant, payload, and a structural framework to which these components are attached.

Presented as Preprint 64-494 at the 1st AIAA Annual Meeting, Washington, D. C., June 29–July 2, 1964; revision received March 22, 1965. This study was supported by NASA Headquarters under Contract NASw-737.

* Analytical Research Engineer. Member AIAA.

† Senior Research Engineer; now with Analytical Mechanics Associates, Cambridge, Mass. Associate Fellow Member AIAA.